



A rationally designed cocatalyst for the Morita–Baylis–Hillman reaction

Charlotte E. S. Jones, Simon M. Turega, Matthew L. Clarke*, Douglas Philp*

EaStCHEM and School of Chemistry, University of St Andrews, North Haugh, St Andrews, Fife KY16 9ST, United Kingdom

ARTICLE INFO

Article history:

Received 8 April 2008

Revised 1 May 2008

Accepted 7 May 2008

Available online 11 May 2008

ABSTRACT

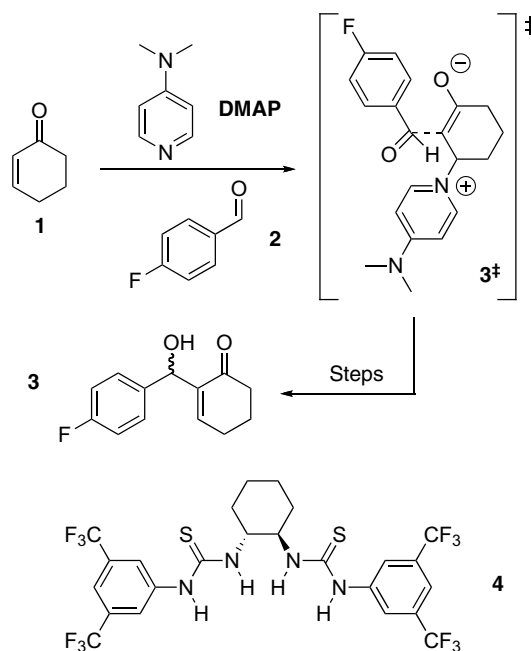
The application of electronic structure calculations to a key transition state in the reaction manifold of the Morita–Baylis–Hillman reaction allows the design of two bis(thiourea) cocatalysts capable of accelerating this reaction through the hydrogen bond mediated recognition of both the nucleophile and the electrophile.

© 2008 Elsevier Ltd. All rights reserved.

The rational design of organic catalysts based on hydrogen bonding¹ is an important objective for the burgeoning field of organocatalysis. We wished to demonstrate that, through the application of electronic structure calculations, it is possible to design a catalyst that is capable of recognising and stabilising a transition state that is assembled from two different reaction partners. In the past, we have shown² that the reactivity of organic molecules can be influenced directly by means of appropriately located recognition elements in the reagents. Further, we³ and others⁴ have shown that both Michael addition reactions and dipolar cycloadditions are amenable to acceleration by exploiting hydrogen bonds formed between a receptor and one of the reagents. Carbon–carbon bond forming reactions mediated by organic catalysts are currently the focus⁵ of many research programmes. Several of these catalysts function by exploiting the fact that hydrogen bond donors can promote reactions in a similar way to Lewis acid catalysts, and there are many excellent examples⁶ of effective catalysts which have been reported to date. Our interest was drawn to the Morita–Baylis–Hillman (MBH) reaction (Scheme 1), since it is one of the more sluggish C–C bond forming reactions that requires more active catalysts in order to realise⁷ its full potential.

We chose to focus on the reaction between cyclohexenone **1** and 4-fluorobenzaldehyde **2** (Scheme 1). The formation of the product **3** can be assayed readily by ¹⁹F NMR spectroscopy, and we were intrigued by the high activity for the elegant bis(thiourea) cocatalyst **4** reported⁸ by Nagasawa and co-workers. These workers propose that in the key step of the MBH reaction, the addition of the DMAP-activated enone to the aldehyde forming the C–C bond, both the aldehyde and enolate are bound and activated by this cocatalyst. We believed that we could increase the activity of this cocatalyst significantly by rational application of computational methods. Through the application of electronic structure methods, we could compute the structure and properties of the transition state **3[‡]**, for the addition of the activated enone to the

aldehyde, and, hence, design a bis(thiourea) cocatalyst which was capable of binding **3[‡]** tightly, thus accelerating the reaction between **1** and **2**. Consideration of the structure of **3[‡]** suggests that any cocatalyst must be capable of simultaneously associating with, and, hence, stabilising both the enolate oxygen arising from the adduct formed between **1** and DMAP and the partial δ^- charge located on the aldehyde carbonyl oxygen atom. As we proceed towards the transition state **3[‡]**, the relative orientations and the charges on these two species will change. Therefore, any cocatalyst design must start from a sound knowledge of the structure and charge distribution present in **3[‡]**.



Scheme 1.

* Corresponding authors. Tel.: +44 1334467264; fax: +44 1334463808 (D.P.).
E-mail address: dp12@st-andrews.ac.uk (D. Philp).

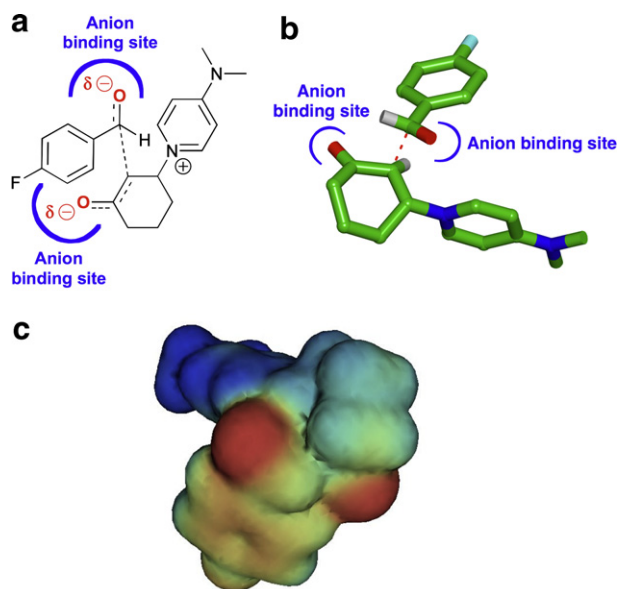


Figure 1. (a) Schematic view of the transition state of the reaction between **1**, activated by **DMAP**, and **2**. The target oxygen atoms are highlighted. (b) Stick representation of the calculated (B3LYP/6-31G(d,p)) structure of 3^\ddagger . Carbon atoms are green, nitrogen atoms are blue, oxygen atoms are red, hydrogen atoms are white and fluorine atoms are cyan. The forming C–C bond is the dashed red line and the location of the anion binding sites are highlighted in blue. Most hydrogen atoms have been omitted for clarity. (c) Electrostatic potential surface of 3^\ddagger . Charge is encoded as a spectrum of red (negative) to blue (positive).

We therefore located and refined the transition state structure of 3^\ddagger using⁹ electronic structure methods. The transition state was initially located (Fig. 1) using a coordinate scan method using the semi-empirical AM1 method as implemented by *AMSOL* 7.1. This transition state structure was then further refined at the B3LYP/6-31G(d,p) level of theory providing us with an accurate model of 3^\ddagger with which to proceed.

The calculated structure of 3^\ddagger reveals (Fig. 1) that, as expected, the regions of highest negative charge are located on the oxygen atoms of **1** and **2**. Interestingly, calculation of the electrostatic potential surface of 3^\ddagger (Fig. 1c) reveals that these two sites carry almost equal negative charge at the transition state, reinforcing the need for both of these sites to be bound and stabilised by any cocatalyst. The two oxygen atoms are placed 4.39 Å apart in the transition state. Interestingly, there is also a C–H···O hydrogen bond (C–H···O distance = 2.39 Å) between the aldehyde carbonyl oxygen and one of the α protons on the pyridine ring of the **DMAP** cocatalyst. As expected, all attempts to dock this transition state structure with the bis(thiourea) cocatalyst **4** such that both of the target oxygen atoms in 3^\ddagger were complexed simultaneously without significant distortion of the calculated transition state structure were unsuccessful.

New cocatalyst designs were generated by placing two thiourea groups at the locations required to recognise the two target oxygen atoms in 3^\ddagger and then connecting them by appropriately sized spacer groups in order to generate approximations to ideal cocatalyst structures. These structures were then refined using molecular mechanics calculations, fixing the atomic positions in 3^\ddagger , but allowing all other atoms to relax. These proposed structures for the transition state bound to the cocatalyst were then optimised using the semi-empirical AM1 method and the SM5.4A⁸ solvation model as before. The results of these calculations (Fig. 2) demonstrated that the transition state structure 3^\ddagger was supported equally well on a cocatalyst that consisted of two thioureas separated by either an *m*-xylyl **5** or an *o*-xylyl **6** bridge.

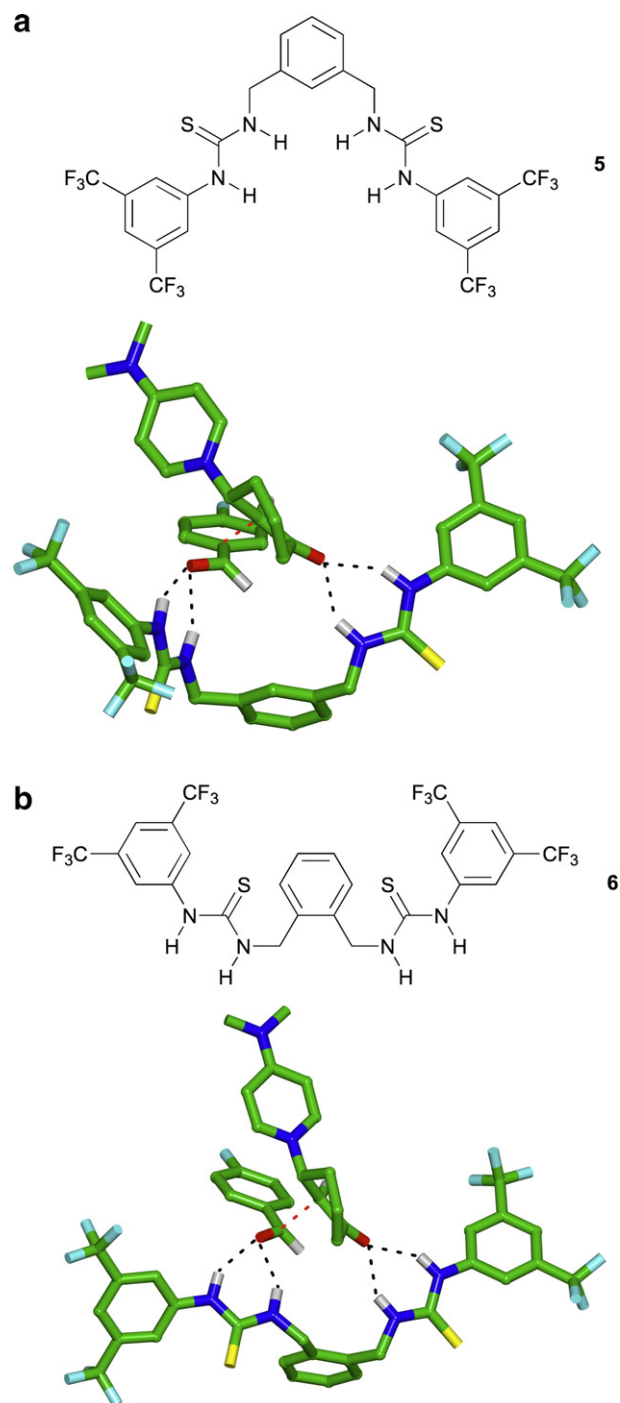


Figure 2. (a) Stick representation of the calculated (AM1/SM5.4a) structure of 3^\ddagger docked to cocatalyst **5**. (b) Stick representation of the calculated (AM1/SM5.4a) structure of 3^\ddagger docked to cocatalyst **6**. In both cases, carbon atoms are green, nitrogen atoms are blue, oxygen atoms are red, sulfur atoms are yellow, hydrogen atoms are white and fluorine atoms are cyan. The forming C–C bond is the dashed red line, and dashed black lines show hydrogen bonds.

Cocatalysts **5** and **6** were then synthesised in 50% and 72% yields, respectively, by reaction of 3,5-bis(trifluoromethyl)phenylisothiocyanate and the appropriate diamine in THF at room temperature.

The ability of the three cocatalysts, **4**, **5** and **6**, to accelerate the reaction between **1** and **2** in the presence¹⁰ of **DMAP** was assessed using a standard set of reaction conditions. In all cases, **1** and **2** were reacted in the absence of solvent. The reaction mixture

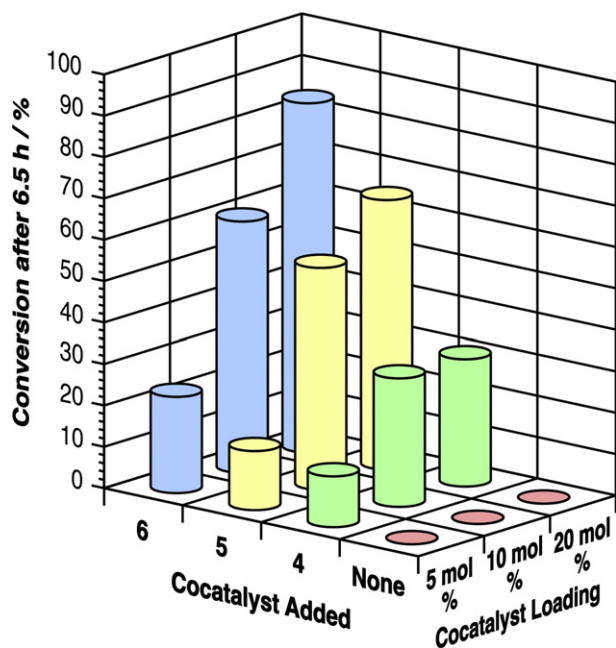


Figure 3. Conversion of ketone **1** and aldehyde **2** to product **3** after 6.5 hours at room temperature in the presence of no cocatalyst (pink) or in the presence of cocatalyst **4** (green), **5** (yellow) or **6** (blue).

contained 1.0 equiv of cyclohexenone **1** and 0.8 equiv of aldehyde **2**. For each of the three cocatalysts, **4**, **5** and **6**, four different cocatalyst loadings were investigated—1 mol %, 5 mol %, 10 mol % or 20 mol %. The ratio of cocatalyst to **DMAP** was held constant and was always 1:1.5. The reaction mixtures were sampled at four time points—after 1.5, 6.5, 32 and 105 h. These samples were diluted with CDCl_3 and the extent of reaction was assessed by 282.3 MHz ^{19}F NMR spectroscopy—deconvolution of the relative areas of the ^{19}F resonance arising from **2** at $\delta -102.3$ and the fluorine resonance arising from the product at $\delta -115.7$ allowed the conversion to be calculated readily. At each cocatalyst loading an additional control experiment was performed where the appropriate amount of **DMAP** was added but no cocatalyst was added. For example, for the 20 mol % cocatalyst loading, the control reaction was performed with no cocatalyst, but with 30 mol % of added **DMAP**.

The results of these screening experiments are summarised in **Figure 3**. It is clear that after 6.5 h, at all **DMAP** concentrations, the reaction between **1** and **2** does not proceed to any measurable extent in the absence of a cocatalyst. The benchmark for the acceleration of the reaction between **1** and **2** is the performance of cocatalyst **4**. After 6.5 h, the reaction requires at least 5 mol % of **4** to be present for any conversion of **1** and **2** to the product **3** to be evident. Increasing the loading of **4** from 5 mol % to 20 mol % increases the conversion from 12% to 31%.

Although cocatalysts **5** and **6** must also be present in at least 5 mol % for any conversion of **1** and **2** to be evident, their ability to accelerate the reaction is much better than **4**. Whilst a loading of 5 mol % of **5** affords a similar conversion (14%) to that observed for **4**, this cocatalyst performs better at higher loadings. The conversion at a loading of 10 mol % is 54% and the conversion rises further to 65% in the presence of 20 mol % of cocatalyst **5**. The best cocatalyst is, however, **6**—increasing the loading of **6** from 5 mol % to 20 mol % increases the conversion from 23% to 84%—almost three times that observed when the reaction is performed under the same conditions in the presence of **4**. After 32 h, there is still no measurable reaction between **1** and **2** in the presence of **DMAP** only. After the same time, in the presence of cocatalyst

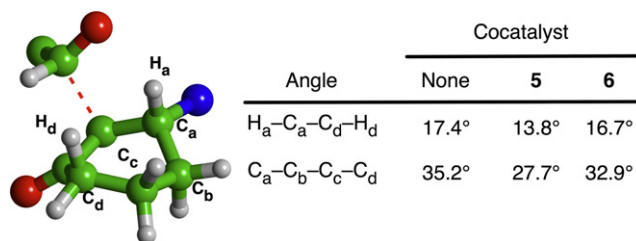


Figure 4. Key angles in the transition states for C–C bond formation in the presence of no cocatalyst and in the presence of cocatalysts **5** and **6**.

4, the conversion ranges from 26% at 5 mol % loading to 82% at 20 mol % loading. In the presence of cocatalysts **5** and **6**, the conversions are uniformly higher—>60% for both cocatalysts at 5 mol % loading and >90% at 20 mol % loading. It is therefore clear that, in agreement with our design, cocatalysts **5** and **6** are both significantly more active than cocatalyst **4**. At a cocatalyst loading of 1 mol %, no product is formed after 6.5 hours in any of the reactions. However, if the reaction mixtures are left at room temperature for 32 h, product is detectable in the reactions containing both cocatalyst **5** (4% conversion) and cocatalyst **6** (2% conversion) indicating that both of these bis(thiourea) cocatalysts retain some activity at low loadings. Screening of other aldehydes as the electrophile in the MBH reaction (see Supporting Information) reveals that the pattern of activity observed with 4-fluorobenzaldehyde is repeated—cocatalyst **6** is between two and three times as active as cocatalyst **4** under the same conditions.

The difference in activity between **5** and **6** is intriguing. Despite their structural similarities, in all experiments, cocatalyst **6** outperforms cocatalyst **5** significantly. A likely explanation for this difference in activity can be found by careful examination of the geometry of the transition state 3^\ddagger bound to each cocatalyst. The cyclohexenone ring adopts a twist boat conformation in the transition state. The geometry of 3^\ddagger bound to cocatalyst **6** is much closer to that calculated for 3^\ddagger in the absence of cocatalyst. When 3^\ddagger is bound to cocatalyst **5**, however, there is a marked departure of the conformation of the cyclohexenone ring towards a true boat geometry. This change in conformation, imposed by the cocatalyst in order to satisfy the steric and electronic requirements of binding, results in an increase in strain within 3^\ddagger resulting in lower activity.

In this Letter, we have demonstrated that it is possible to use electronic structure calculations to design two cocatalysts that are capable of recognising a key transition state within the reaction manifold of the Morita–Baylis–Hillman reaction. These cocatalysts are capable of increasing the rate of the target reaction by a factor of three and retain some activity even at very low (1 mol %) loadings. We believe that the design strategy presented here may be of significant utility in the design and optimisation of new organic cocatalysts that utilise hydrogen bonding.

Acknowledgements

We thank the Engineering and Physical Sciences Research Council and the University of St Andrews for financial support.

Supplementary data

Supplementary data contain synthetic procedures and characterisation data for compounds **3**, **5** and **6**. Details of the reactions of other aldehydes using cocatalysts **4** and **6**. Coordinates for the calculated transition states shown in **Figures 1** and **2**. Supplementary data associated with this article can be found, in the online version, at doi:10.1016/j.tetlet.2008.05.037.

References and notes

- (a) Taylor, M. S.; Jacobsen, E. N. *J. Am. Chem. Soc.* **2004**, *126*, 10558; (b) Dove, A. P.; Pratt, R. C.; Lohmeijer, B. G. G.; Waymouth, R. M.; Hedrick, J. L. *J. Am. Chem. Soc.* **2005**, *127*, 13798; (c) Fuerst, D. E.; Jacobsen, E. N. *J. Am. Chem. Soc.* **2005**, *127*, 8964; (d) Okino, T.; Hoashi, Y.; Takemoto, Y. *J. Am. Chem. Soc.* **2003**, *125*, 12672.
- (a) Kassianidis, E.; Pearson, R. J.; Philp, D. *Chem. Eur. J.* **2006**, *12*, 6829; (b) Pearson, R. J.; Kassianidis, E.; Slawin, A. M. Z.; Philp, D. *Chem. Eur. J.* **2006**, *12*, 8788; (c) Pearson, R. J.; Kassianidis, E.; Philp, D. *Org. Lett.* **2005**, *7*, 3833; (d) Pearson, R. J.; Kassianidis, E.; Slawin, A. M. Z.; Philp, D. *Org. Biomol. Chem.* **2004**, *2*, 3434.
- (a) Ashton, P. R.; Calcagno, P.; Spencer, N.; Harris, K. D. M.; Philp, D. *Org. Lett.* **2000**, *2*, 1365; (b) Rowe, H. L.; Spencer, N.; Philp, D. *Tetrahedron Lett.* **2000**, *41*, 4475.
- (a) Kelly, T. R.; Meghani, P.; Ekkundi, V. S. *Tetrahedron Lett.* **1990**, *31*, 3381; (b) Curran, D. P.; Kao, L. H. *J. Org. Chem.* **1994**, *59*, 3259; (c) Curran, D. P.; Kao, L. H. *Tetrahedron Lett.* **1995**, *36*, 6647; (d) Schreiner, P. R.; Wittkopp, A. *Org. Lett.* **2002**, *4*, 217; (e) Wittkop, A.; Schreiner, P. R. *Chem. Eur. J.* **2003**, *9*, 407.
- For recent reviews see: (a) Dalko, P. I.; Moisan, L. *Angew. Chem., Int. Ed.* **2001**, *40*, 3726; (b) Schreiner, P. R. *Chem. Soc. Rev.* **2003**, *32*, 289; (c) Dalko, P. I.; Moisan, L. *Angew. Chem., Int. Ed.* **2004**, *43*, 5138; (d) Seayad, J.; List, B. *Org. Biomol. Chem.* **2005**, *3*, 719; (e) Takemoto, Y. *Org. Biomol. Chem.* **2005**, *3*, 4299; (f) Taylor, M. S.; Jacobsen, E. N. *Angew. Chem., Int. Ed.* **2006**, *55*, 1520.
- For reviews, see: (a) Schreiner, P. R. *Chem. Soc. Rev.* **2003**, *32*, 289; (b) Pihko, P. M. *Angew. Chem., Int. Ed.* **2004**, *43*, 2062; For hydrogen bond promoted Morita-Baylis–Hillman reactions, see: (c) Wang, J.; Li, H.; Yu, X.; Zu, L.; Wang, W. *Org. Lett.* **2005**, *7*, 4293; (d) Maher, D. J.; Connon, S. J. *Tetrahedron Lett.* **2004**, *45*, 1301.
- (a) Aggarwal, V. K.; Mereu, D. K.; Williams, R. J. *Org. Chem.* **2002**, *67*, 510; (b) Aggarwal, V. K.; Emme, I.; Fulford, S. Y. *J. Org. Chem.* **2003**, *68*, 692; (c) Santos, L. S.; Pavam, C. H.; Almeida, W. P.; Coelho, F.; Eberlin, M. N. *Angew. Chem., Int. Ed.* **2004**, *43*, 4330; (d) Aggarwal, V. K.; Fulford, S. Y.; Lloyd-Jones, G. C. *Angew. Chem., Int. Ed.* **2005**, *44*, 26; (e) Price, K. E.; Broadwater, S. J.; Jung, H. M.; McQuade, D. T. *Org. Lett.* **2005**, *7*, 147; (f) Price, K. E.; Broadwater, S. J.; Walker, B. J.; McQuade, D. T. *J. Org. Chem.* **2005**, *70*, 3980; (g) Basavaiah, D.; Rao, A. J.; Satyanarayana, T. *Chem. Rev.* **2003**, *103*, 811.
- Sohtome, Y.; Tanatani, A.; Hashimoto, Y.; Nagasawa, K. *Tetrahedron Lett.* **2004**, *45*, 5589.
- All SM5.4A/AM1 calculations were performed using AMSOL 7.1 running on a Linux cluster. (AMSOL Ver. 7.1 by G. D. Hawkins, D. J. Giesen, G. C. Lynch, C. C. Chambers, I. Rossi, J. W. Storer, J. Li, J. D. Thompson, P. Winget, B. J. Lynch, D. Rinaldi, D. A. Liotard, C. J. Cramer, D. G. Truhlar; EF routines by F. Jensen). All molecular mechanics calculations were carried out using the AMBER or MMFFs force field as implemented in MACROMODEL (Ver. 9.5; Schrödinger, Inc.: Portland, OR, 2007) running on a Linux workstation. DFT calculations were performed using GAMESS (Ver. dated 24 March 2007, Rev 3). Schmidt, M. W.; Baldrige, K. K.; Boatz, J. A.; Elbert, S. T.; Gordon, M. S.; Jensen, J. H.; Koseki, S.; Matsunaga, N.; Nguyen, K. A.; Su, S. J.; Windus, T. L.; Dupuis, M.; Montgomery, J. A. *J. Comput. Chem.* **1993**, *14*, 1347.
- There is no measurable reaction between **1** and **2** under the conditions employed in this work in the absence of **DMAP** or in the presence of 30 mol % **DMAP** and 20 mol % of a mono(thiourea), 3,5-bis(trifluoromethyl)phenylbenzylthiourea.